Experimental analyzis of the effect of electromagnetic stirring on the solidification process of the Sn-10wt.%Pb alloy

L Hachani, K Zaidat, Y Fautrelle

Experimental analyzis of the effect of electromagnetic stirring on the solidification process of the Sn-10wt.%Pb alloy.

L. Hachani[1], K. Zaidat[2], Y. Fautrelle[2]

[1] Laboratoire de physique des matériaux, Université Amar Telidji de Laghouat, Algérie
[2] Laboratoire SIMAP-EPM, Université de Grenoble, BP 75, 38402 Saint Martin d'Hères, France

Corresponding author: lakhdar.hachani@yahoo.fr

Abstract
A comparative study of solidification experiments for three modes of electromagnetic stirring is conducted on a benchmark experiment model. The goal of this work is to analyse the effect of different forced convection by changing the direction of the Lorentz force on the solidification process with respect to different aspects: thermal, structure, and morphology of segregation. Experimental results consist of instantaneous temperature maps provided by a lattice of 50 thermocouples welded on the large crucible side and post-mortem characterizations of the samples, such as X-ray imaging and metallography. Results show that forced convection promotes equiaxed structures, the fluid flow pattern influences grain size according to its direction with respect to natural convection. However, the results show that all electromagnetic stirring modes effectively reduce macrosegregations significantly, while remaining inactive for reducing development of segregated channels.

Key words:
Solidification, Natural and forced convection, Benchmark experiment, Macrostructure, Freckles, Segregations, Electromagnetic stirring, Lorentz force

1. Introduction

Rigorous control of the solidification is one of the main targets in metallurgical process. This control aims to suppress the defects as well as improving the final properties of the solidified ingot. It has been widely accepted that the convective motions are responsible for various kinds of phenomena, like macro/meso-segregations, remelting, dendrite fragmentation and promotion of equiaxed structures [1]. Electromagnetic stirring is a well-established high efficiency technique, to stir the bulk and the mushy zone during the solidification step in order to homogenize the composition in the liquid. The consequences are improvements of the quality and productivity of final ingot. The use of travelling magnetic fields (TMF) in the solidification process has shown its effectiveness to control the convection so as to reduce various defects related to the heterogeneity and increase the equiaxed grain zone [2-5]. In opposition, the static magnetic field is used to decrease the level of fluid flows for example in order to eliminate natural convection in crystal growth [6-8]. It has been demonstrated that by means of intense static fields it is also possible to produce crystal alignment, morphology of structures or phase sedimentation [9-10], however, it was realized quite recently that static magnetic fields may interact with thermo-electric current and produces flows, the so-called magneto-thermo-electric currents [11]. This work proposes to investigate experimentally the effect of various types of electromagnetic stirring on the solidification of a model alloy (Sn–10wt.%Pb). The effect of the forced convection driven by a traveling magnetic field on the solidification process will be study in terms of temperature history, structures and solute distribution in the final solid sample. Three cases of stirring were investigated: in the same direction as natural convection, reversed with respect to natural convection, and periodically reversed with a modulation frequency equal to 0.125 Hz.

2. Experimental process

The experiment consists in solidifying a rectangular ingot of Sn–10wt.%Pb alloy by using two lateral heat exchangers, allowing extraction of the heat flux from one or two vertical sides of the sample. The domain is a quasi-two dimensional rectangular ingot (100×60×10 mm). The temperature difference ΔT between the two lateral sides is 40 K, and the cooling rate CR = 0.03 K/s. The instrumentation consists in recording the instantaneous temperature maps each second by means of a lattice of 50 thermocouples. The reader is referred to the works [14-15] for further details concerning the description of an identical experimental setup. The electromagnetic force is imposed during the whole experimental process, i.e., from the beginning of sample melting to the end of solidification. Four types of electromagnetic stirring conditions were investigated (see Fig. 1).

Case I: the melt is solidified under natural convection (without stirring). The temperature difference between the two lateral sides of the sample produces a clockwise eddy flow (Fig. 1(a)), where the cold wall is located on the right.

Case II: the experimental conditions are the same as in Case I with an additional electromagnetic force imposed in the same direction as natural convection. The direction of the flow is also in the clockwise direction (see Fig. 1(b)).

Case III: the experimental conditions are the same as in Case I, but the electromagnetic force direction is reversed with respect to natural convection as presented in Fig. 1(c).
Case IV: the experimental conditions are the same as in Case I, but the electromagnetic force direction is periodically reversed. Electromagnetic force inversion frequency is equal to 0.125 Hz as illustrated in Fig. 1(d).

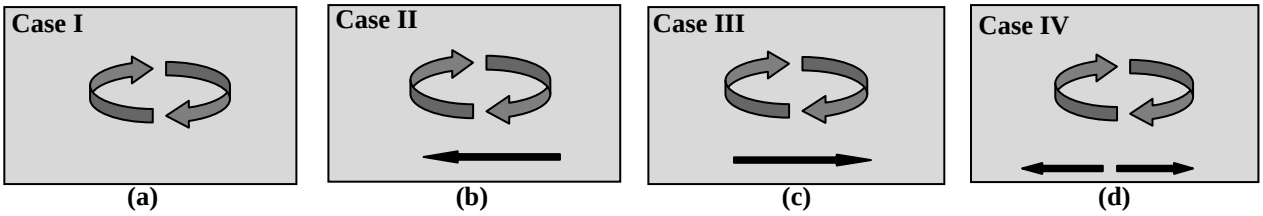

Fig. 1. The different electromagnetic stirring modes compared to the direction of thermosolutal convection.

3. Results and discussion

3.1. Temperature field evolution

Fig. 2 shows instantaneous temperature maps coupled with vectors indicating the local thermal gradients for the different solidification cases discussed above (Cases I, II, III and IV) at time t = 16800 s, which corresponds to a period of 10 minutes after the start of the solidification phase. In the stirred cases, coil intensity is I = 8.2 A. The temperature gradients were calculated at each thermocouple location from the temperature difference between two adjacent points by means of a centred difference numerical scheme. The arrows correspond to the $-\vec{\nabla}T$ vector, which is proportional to local heat flux density. We denote by DT the temperature difference between the maximum temperature and the minimum temperature in each case ($DT = T_{max} - T_{min}$). When forced convection is imposed, DT decreases from 18.7 K in the Case I to 15 K, 14.9 K and 10.2 K respectively in Cases II, III and IV, respectively. This may likely be attributed to the mixing effect induced by the electromagnetic stirring. However, under stirring conditions the minimum temperature T_{min} is higher than in the thermosolutal case (see Fig. 2(a)). The temperature maps clearly shows the effect of electromagnetic stirring on temperature distribution, namely homogenization of temperature in the melt as well as modifies the fluid flow configuration. A comparative study at this instant shows that stirring in the same direction as thermosolutal convection (Case II) is greatly strengthens convection (Fig. 2(a) and (b)). We noticed that in Case III the second stirring mode (stirring in the opposite direction to convection) modifies flow configuration significantly. This is shown by deformation of the isotherms, meaning that a vortex appears in the opposite direction with respect to thermosolutal convection. However, periodically reverse stirring (Case IV) seems to create two small vortices of different directions. The first is located on the left side with a direction similar to natural convection, while the second is activated on the right side (cold side) with an opposite direction. We recall that in Case IV the frequency of stirring direction changes is f = 0.125 Hz. Indeed, this choice was adopted to ensure sufficient time for convection to transport solutal elements at a considerable distance from the mushy zone to the liquid bath, but without exceeding the time required for development of a channel (time segregation), [16–17].

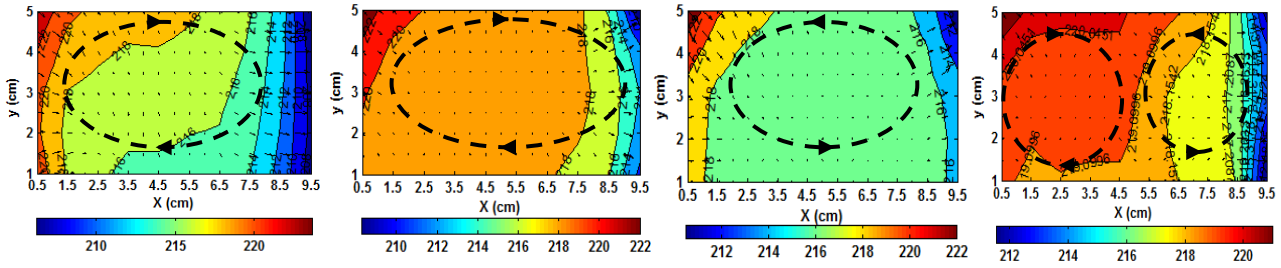

Case I
T_{max} = 221.42°C; T_{min} = 202.72°C
DT = 18.7°C

Case II
T_{max} = 222.56 °C; T_{min} = 207.56°C
DT = 15°C

Case III
T_{max} = 222.43 °C; T_{min} = 208.73 °C
DT = 14.9°C

Case IV
T_{max} = 222.83 °C; T_{min} = 212.63 °C
DT = 10.2 °C

Fig. 2. Instantaneous temperature maps with superimposed local temperature gradient vectors ($-\vec{\nabla}T$) for the four solidification cases at t = 16800 s. The experimental conditions are: Sn-10wt%Pb alloy, ΔT = 40 K, CR = 0.03 K/s, inductor current I = 8.2A.

3.2. Effect of electromagnetic stirring on grain structures

In order to examine the effect of different electromagnetic stirring modes applied on the final metallographic structure. We polished and revealed the final ingot in order to study grain size, macrostructures of ingots obtained from four solidification cases, (the treatment procedure is detailed in the work [15]). Fig. 3(a) shows the macrostructure of the Sn–

10wt.%Pb ingot solidified under the effect of thermosolutal convection only. We observe that the dominant morphology of the macrostructure in this case is columnar with an equiaxed zone corresponding to the last liquid at the end of solidification. The upwind tilting of the columnar grains is consistent with the direction of natural convection. Fig. 3(b) shows the case of solidification under a stirring in the same direction of the natural convection. We notice that the area of the columnar region has regressed. Moreover, the equiaxed area has increased significantly. This result can be attributed to electromagnetic stirring that exerts two main effects. First, the Lorentz force generates liquid metal convection that homogenizes the pool and the temperature gradients are lower than the previous case, thereby creating favourable conditions for appearance of a CET. Second, a hot flow impinging the solid–liquid interface can enhance fragmentation/remelting of the secondary arms. Transported by convection, under certain conditions these fragments can give equiaxed grains. The case in the opposite direction to thermosolutal convection is shown in Fig. 3(c). The structure mainly consists of fine size equiaxed grains. A small columnar region is located in the bottom right angle of the ingot. It is important to note that the efficiency of electromagnetic stirring in refining the structure is improved significantly when we reversed the direction of stirring against natural convection. In parallel with the mechanical fragmentation effect, this stirring mode seems to have a significant consequence on the dendrite remelting process. Indeed, stirring generates an upward motion of lead-enriched liquid along the columnar front in this case. Fig. 3(d) shows the case of solidification under periodically reversed stirring with a reversal frequency of 0.125 Hz (Case IV). This case also presents a predominant equiaxed structure. The columnar region is restricted to the two right-hand corners on the cold side.

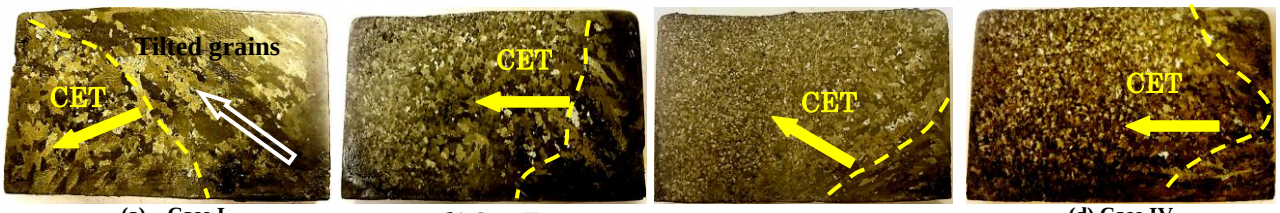

(a) Case I
Without electromagnetic stirring

(b) Case II
Stirring in the same direction as natural convection.

(c) Case III
Stirring in the opposite direction to natural convection

(d) Case IV
Periodically reversed stirring (reversal f = 0.125Hz)

Fig. 3. Macrostructure on the lateral plane of different ingots of Sn–10 wt.%Pb. The experimental conditions are: temperature difference DT = 40 K, cooling rate CR = 0.03 K/s and the applied current intensity I = 8.2 A.

3.3. Effect of electromagnetic stirring on meso- and macrosegregation

In order to analyse quantitatively the effect of different electromagnetic stirring modes on lead concentration distribution, an X-ray analysis of the samples was performed (CEA/DIMRI, Saclay France). The composition maps presented in Fig.4 were built from the digitalized images. The X-ray images confirm the existence of several segregation modes. Segregated channels are located on the right part of all samples in the columnar region; whereas macrosegregation zones, corresponding to the last liquid solidified, are always located in the bottom left side of the samples. Segregated channel dimensions are several centimetres in length and a few millimetres in width. Fig. 4(a) shows the solidification case of Sn–10wt.%Pb under natural convection. A wide segregation zone is observed at the bottom left side of the ingot, with a concentration greater than 20%. A small mesosegregation is located in the right-hand corner, probably due to the presence of several channels at this point. We notice that, in this case, the segregated channels have an oblique geometry and a level of concentration ranging between 11% and 12%.

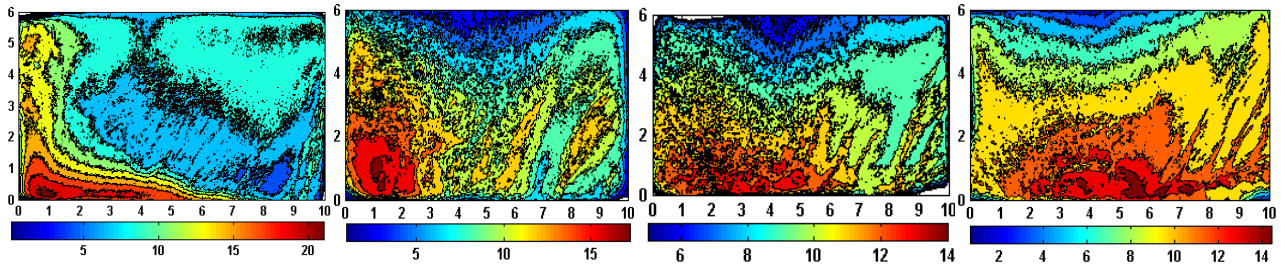

(a) Case-I **(b) Case-II** **(c) Case-III** **(d) Case-IV**

Fig. 4. X-ray photos digital processing of four solidified ingots showing the different types of meso and macrosegregation. The alloy is Sn–10wt.%Pb.

The X-radiography of the ingot solidified under the effect of electromagnetic stirring in the same direction of thermosolutal convection is shown in Fig. 4(b). A decline in the macrosegregation zone, corresponding to the last liquid (left region) with a level concentration ranging between 15% and 18%, was observed. This could be accounted by the fact that structures are mainly equiaxed in that region, as indicated in Fig. 3. Consequently, the draining flow is likely to be significantly different compared to the natural convection case. Furthermore, this stirring mode promotes penetration of liquid from the hot bulk into the mushy zone by increasing the both effect of pumping solutal elements into the interdendritic liquid and of secondary remelting of dendritic arms.Therefore, meso and macrosegregation occur at the same time as increase in channel segregated sizes. Digital images processing of X-ray radiography of the ingot clearly shows a significant increase in concentration of segregated channels ranging between 12% and 14%. The case of stirring in the opposite direction to thermosolutal convection is shown in Fig. 4(c). We note that the macrosegregation area is smaller than in the previous cases, and is located in the centre of the ingot. This segregation zone has a concentration level lesser than the natural case, ranging between 13% and 14%. Fig. 4(d) shows the case of the last electromagnetic stirring mode (stirring with a reversal frequency of 0.125 Hz). It is clear that this stirring mode promotes formation of segregated channels in size and number. However we found that, unlike the previous cases, the extension of regions with high positive segregation is lesser than the natural case. Indeed, the reversal time of 8 seconds is greater than the necessary transit time of the convective flow in the mushy zone (see for example [17]). Note that the granulation occurring in the equiaxed zone is more pronounced than in the other stirred cases. It is not easy to conclude since the image corresponds to an integration of the X-ray beam through the thickness of the sample.

4. Conclusions

Through this experimental study, we can deduce some findings and general conclusions about the effect of different electromagnetic stirring modes on the solidification process of Sn-10wt.%Pb alloy. Indeed, the different segregation morphologies are substantially generated by the fluid flow in the mushy zone. Electromagnetic stirring in the direction of thermosolutal convection does not remove the segregated channels. Stirring can even create and promote segregation. The positions of segregated channels are directly related to the flow pattern generated by the applied electromagnetic force. The observations show that the channel morphology in transverse cross-sections may be complex. However, a significant change in the macrostructure was observed particularly with regard to the columnar-equiaxed transition (CET). Stirring in the opposite direction of the natural convection has shown its effectiveness in achieving the finest equiaxed structures on almost all ingots. In the case of periodically reversed stirring with reversal frequency f = 0.125 Hz, we observed an identical effect in the case of stirring in the opposite direction to convection, namely a predominantly equiaxed structure, a decrease in stratification of the solutal element, and formation of high concentration and large-size segregated channels.

References

[1] C.J. Paradies, R.N. Smith, M.E. Glicksman (1997), Metall. Mater. Trans A, 28A, 875-883.
[2] M. Medina, Y. Du Terrail, F. Durand, Y. Fautrelle (2004), Metall. Mater. Trans. B 35 (4), 743–755.
[3] B. Willers, S. Eckert, U. Michel, I. Haase, G. Zouhar (2005), Mater. Sci. Eng. A 402 (1–2), 55–65.
[4] A. Noeppel, A. Ciobanas, X.D. Wang, K. Zaidat, N. Mangelinck, O. Budenkova, A. Weiss, G. Zimmermann, Y. Fautrelle (2010), Metall. Mater. Trans. B 41 (1), 193–208.
[5] L. Hachani, K. Zaidat, Y. Fautrelle (2015), Int. J. Heat and Mass Transfer. 85, 438-454.
[6] A.J. Mikelson, J. Karklin (1981), J. Cryst. Growth. 52, 524-529.
[7] L.A. Gorbunov (1988), Magnetohydrodynamics. 4, 404-406.
[8] Yu. Gelfgat, L.A. Gorbunov (1989), Sov. Phys. Dokl. 34, 470-472.
[9] X. Li, Y. Fautrelle, Z.-M. Ren (2007), Acta Mater. 55, 1377-1386.
[10] X. Li, Y. Fautrelle, Z.-M. Ren (2007), Acta Mater. 55, 3803-3813.
[11] X. Li, Y. Fautrelle, K. Zaidat, A. Gagnoud, Z.-M. Ren, Y.-D. Chang, R. Moreau, C. Esling (2010), J. Crystal Growth. 312, 267-272.
[12] D.J. Hebditch, J.D. Hunt (1974). Metall. Trans. 5, 1557–1563.
[13] G. Quillet, A. Ciobanas, P. Lehmann, Y. Fautrelle (2007), Int. J. Heat Mass Transfer 50 (3–4), 654–666.
[14] X.D. Wang, Y. Fautrelle (2009), Int. J. Heat Mass Transfer 52 (23–24), 5624–5633.
[15] L. Hachani, B. Saadi, X.D. Wang, A. Nouri, K. Zaidat, A. Belgacem-Bouzida, L. Ayouni-Derouiche, G. Raimondi, Y. Fautrelle (2012), Int. J. Heat Mass Transfer 55 (7–8), 1986–1996.
[16] X.D. Wang, Y. Fautrelle, J. Etay, R. Moreau (2009), Metall. Mater. Trans. B 40 (1), 82–90.
[17] X.D. Wang, Y. Fautrelle, J. Etay, R. Moreau (2009), Metall. Mater. Trans. B 40 (1), 104–113.